

263
5-23-79

DR. 2606

ORNL/TM-6782

Influence of Melting Practice and Heat Treatment on the Continuous Cycling Fatigue and Subcritical Crack Growth Properties of 2 $\frac{1}{4}$ Cr-1 Mo Steel

J. P. Strizak
C. R. Brinkman

MASTER

APPLIED TECHNOLOGY

Any further distribution by any holder of this document or of the data therein to other parties representing foreign interests, foreign governments, foreign companies and foreign subsidiaries or foreign divisions of U.S. companies should be coordinated with the Director, Division of Reactor Research and Technology, Department of Energy.

OAK RIDGE NATIONAL LABORATORY
OPERATED BY UNION CARBIDE CORPORATION · FOR THE DEPARTMENT OF ENERGY

XXXXX

DISCLAIMER

This report was prepared as an account of work sponsored by an agency of the United States Government. Neither the United States Government nor any agency Thereof, nor any of their employees, makes any warranty, express or implied, or assumes any legal liability or responsibility for the accuracy, completeness, or usefulness of any information, apparatus, product, or process disclosed, or represents that its use would not infringe privately owned rights. Reference herein to any specific commercial product, process, or service by trade name, trademark, manufacturer, or otherwise does not necessarily constitute or imply its endorsement, recommendation, or favoring by the United States Government or any agency thereof. The views and opinions of authors expressed herein do not necessarily state or reflect those of the United States Government or any agency thereof.

DISCLAIMER

Portions of this document may be illegible in electronic image products. Images are produced from the best available original document.

Printed in the United States of America. Available from
the Department of Energy,
Technical Information Center
P.O. Box 62, Oak Ridge, Tennessee 37830
Price: Printed Copy \$4.50 ; Microfiche \$3.00

This report was prepared as an account of work sponsored by an agency of the United States Government. Neither the United States Government nor any agency thereof, nor any of their employees, contractors, subcontractors, or their employees, makes any warranty, express or implied, nor assumes any legal liability or responsibility for any third party's use or the results of such use of any information, apparatus, product or process disclosed in this report, nor represents that its use by such third party would not infringe privately owned rights.

ORNL/TM-6782
Distribution
Category UC-79b, -h, -k

Contract No. W-7405-eng-26

METALS AND CERAMICS DIVISION

INFLUENCE OF MELTING PRACTICE AND HEAT TREATMENT ON THE
CONTINUOUS CYCLING FATIGUE AND SUBCRITICAL CRACK GROWTH
PROPERTIES OF 2 1/4 Cr-1 Mo STEEL

J. P. Strizak and C. R. Brinkman

Date Published - May 1979

NOTICE This document contains information of a preliminary nature.
It is subject to revision or correction and therefore does not represent a
final report.

OAK RIDGE NATIONAL LABORATORY
Oak Ridge, Tennessee 37830
operated by
UNION CARBIDE CORPORATION
for the
DEPARTMENT OF ENERGY

Blank Page

CONTENTS

ABSTRACT	1
INTRODUCTION	1
MATERIAL CHARACTERIZATION AND EXPERIMENTAL PROCEDURES	2
RESULTS AND DISCUSSION	7
Strain-Controlled Continuous Cycling Fatigue	7
Fatigue Crack Growth Rate	14
CONCLUSIONS	18
ACKNOWLEDGMENTS	19
REFERENCES	19
APPENDIX	23

NOTICE

This report was prepared as an account of work sponsored by the United States Government. Neither the United States nor the United States Department of Energy, nor any of their employees, nor any of their contractors, subcontractors, or their employees, makes any warranty, express or implied, or assumes any legal liability or responsibility for the accuracy, completeness or usefulness of any information, apparatus, product or process disclosed, or represents that its use would not infringe privately owned rights.

INFLUENCE OF MELTING PRACTICE AND HEAT TREATMENT ON THE
CONTINUOUS CYCLING FATIGUE AND SUBCRITICAL CRACK GROWTH
PROPERTIES OF 2 1/4 Cr-1 Mo STEEL*

J. P. Strizak and C. R. Brinkman

ABSTRACT

Interim results are reported for continuous cycling strain-controlled fatigue and fatigue crack growth tests of 2 1/4 Cr-1 Mo steel. Heat-to-heat variations due to different melting practices and postweld heat treatment of annealed and isothermally annealed material were considered. Apparently, continuous cycle fatigue behavior at 427 and 538°C did not differ among the heats manufactured by air-melt, vacuum-arc remelt, and electro-slag remelt practices. Furthermore, a possible postweld heat treatment of 40 h at 726°C on initially annealed or isothermally annealed material did not influence continuous cycle fatigue life. Interim fatigue crack growth rate results at 510°C extended data to higher stress intensity levels. Fatigue crack growth rate data for isothermally annealed air-melt material obtained at frequencies of 0.067 and 0.67 Hz over a stress intensity range of 30 to 60 MPa \sqrt{m} agreed well with previous results not exceeding 40 MPa \sqrt{m} . Cyclic life tests using both hourglass-shaped and uniform-gage specimens were compared. The 5.08-mm-diam hourglass-shaped specimen had a lower fatigue life than the 6.35-mm specimen. The discrepancy in the results for these two hourglass-shaped specimens decreases with decreasing total axial strain range. Furthermore, the uniform-gage specimen had a lower fatigue life than the 6.35-mm-diam hourglass-shaped specimen.

INTRODUCTION

The candidate material for construction of fast breeder reactor steam generators for nuclear power generating systems such as the Clinch River Breeder Reactor (CRBR) is 2 1/4 Cr-1 Mo steel. Present plans for the CRBR call for use of air-melt heats for shell components, vacuum-arc remelt (VAR) material for tubesheet forgings, and electro-slag remelt (ESR) material for tubing. Thus, the effects of melting practice, composition

*Work performed under DOE/RRT 189a OH050, Mechanical Properties for Structural Materials.

or heat-to-heat variations, thermal-mechanical processing history, and postweld heat treatment (PWHT) of annealed and isothermally annealed material on the mechanical properties of 2 1/4 Cr-1 Mo steel are of concern in steam generator design. Our objective is to investigate these factors and their effects on the strain-controlled fatigue and fatigue crack growth of 2 1/4 Cr-1 Mo steel.

MATERIAL CHARACTERIZATION AND EXPERIMENTAL PROCEDURES

Specimens for the ongoing continuous cycling fatigue and fatigue crack growth investigations came from commercial heats of 2 1/4 Cr-1 Mo steel. Heat numbers, vendor sources, product forms, and heat treatments of the air-melt, VAR, and ESR heats before specimen fabrication are listed in Table 1. Table 2 gives the chemical compositions of the

Table 1. 2 1/4 Cr-1 Mo Steel for Fatigue and Crack Growth Test Specimens

Heat	Vendor	Melting practice	Product form	Heat treatment	Specimen type
3P5601	Babcock and Wilcox Company	air	25.4-mm Plate, ASME SA-387, Grade D	Anneal + PWHT	Fatigue
56447	Republic Steel Company	VAR	51-mm Plate ^a	Anneal + PWHT	Fatigue
91775	Babcock and Wilcox Company	ESR	22-mm bar ^b	Isothermal Anneal + PWHT	Fatigue
C-6534-10H	Babcock and Wilcox Company	air	25-mm Plate, ASME SA-387, Grade D	Isothermal Anneal	Crack growth

^aProduced from forging (ASME SA 336) made by Cameron Iron Works. Plate cut to 25.4-mm square blocks prior to heat treatment.

^bSwaged down from 29-mm bar stock originally hot extruded from 102 × 102-mm ESR billet.

Table 2. Chemical Compositions of 2 1/4 Cr-1 Mo Steel

Heat	Content, wt %							
	C	Mn	Si	Cr	Mo	Ni	S	P
3P5601	0.12	0.35	0.27	2.30	0.96	0.20	0.022	0.009
56447	0.098	0.53	0.22	2.20	1.03	0.24	0.005	0.059
91775	0.103	0.46	0.32	2.30	1.01	0.04	0.004	0.010

various heats. Fatigue specimens were fabricated from heat-treated air-melt, VAR, and ESR material, which was either isothermally annealed or annealed and subsequently postweld heat-treated, as described in Table 3. Both the hourglass-shaped and uniform-gage specimens shown in Fig. 1 were machined with the longitudinal axis parallel to the length of the bar stock or the rolling direction of the plate.

Table 3. Heat Treatments of Tested Materials

Heat	Description
3P5601 and 56447	Anneal: Austenitize at 927°C for 1 h; cool to 316°C at ~56°C/h; air cool to room temperature. PWHT: Heat to 726°C; hold for 40 h; cool to 316°C at ~56°C/h; air cool to room temperature.
C-6534-10H	Isothermal Anneal: Austenitize at 927°C for 1 h; cool to 704°C at ~84°C/h; hold at 704°C for 2 h; cool to room temperature at ~36°C/h.
91775	Isothermal Anneal: Same as heat C-6539-10H. PWHT: Same as 3P5601 and 56447.

Compact tension specimens (Fig. 2) were used for subcritical crack growth testing. The specimens were fabricated from air-melt material (heat C-6534-10H), which had been isothermally annealed as described in Table 3. The specimen thickness (B) was centered in the 25-mm plate, and the notch was oriented so that crack growth would be parallel to the rolling direction (ASTM E 399, T-L orientation).

Fully reversed push-pull fatigue tests were conducted in a closed-loop electrohydraulic fatigue test machine. Axial strain control was maintained for the hourglass-shaped specimens with a diametral

ORNL-DWG 78-18337

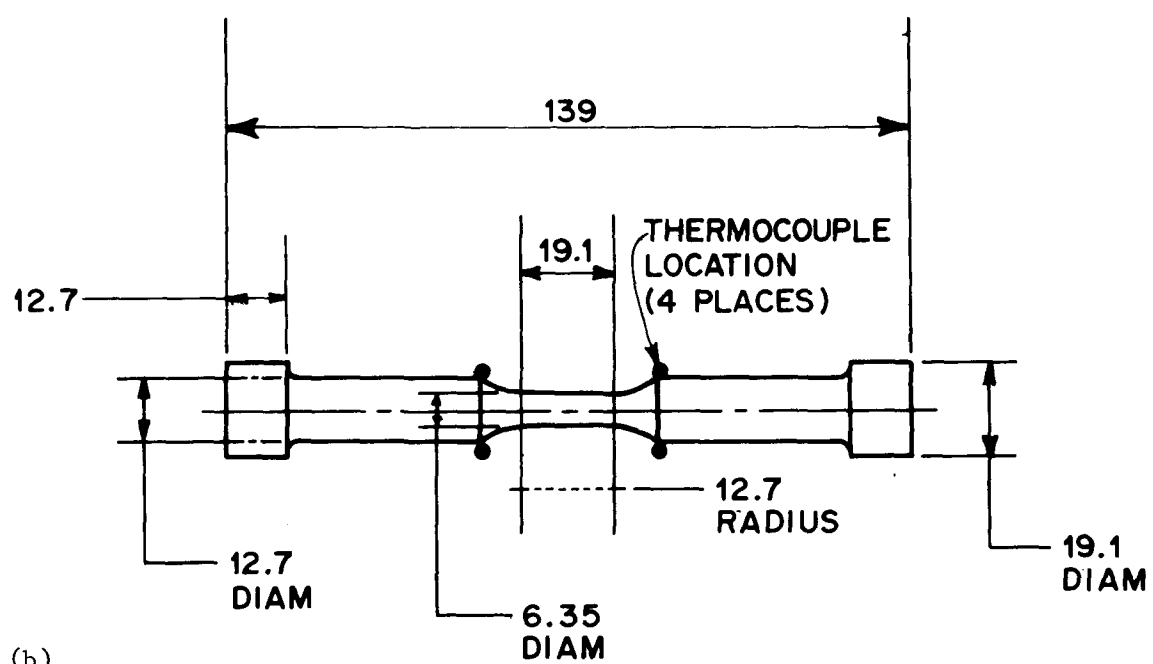
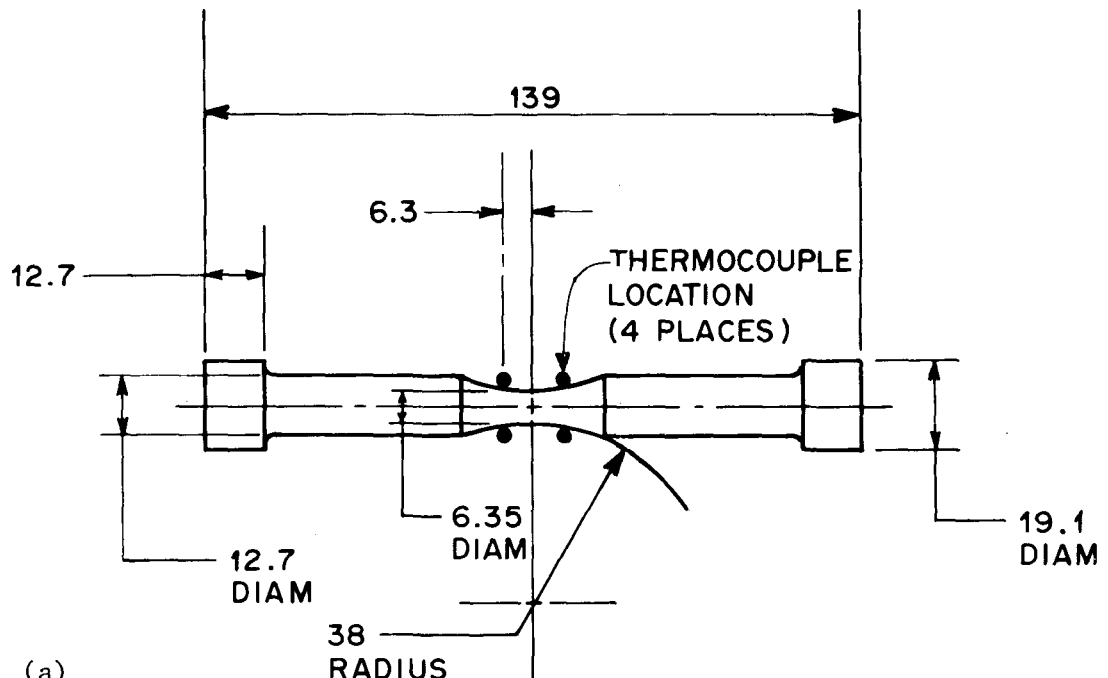


Fig. 1. Strain- and Load-Controlled Fatigue Specimens.
(a) Hourglass specimen. (b) Uniform-gage specimen. Dimensions in millimeters.

ORNL-DWG 78-18336

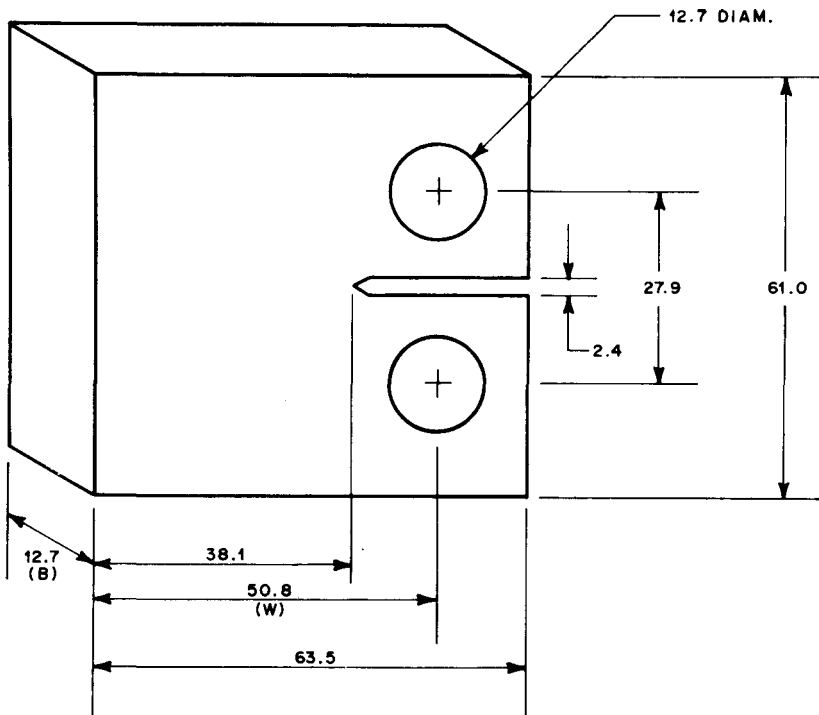


Fig. 2. Compact Tension Fatigue Crack Growth Specimen. Dimensions in millimeters.

extensometer, load cell, and a simple diametral-to-axial strain computer. Axial strain was measured and controlled directly with an axial extensometer for uniform-gage specimens. A triangular waveform as shown in Fig. 3 was used for all tests.

ORNL-DWG 75-11066

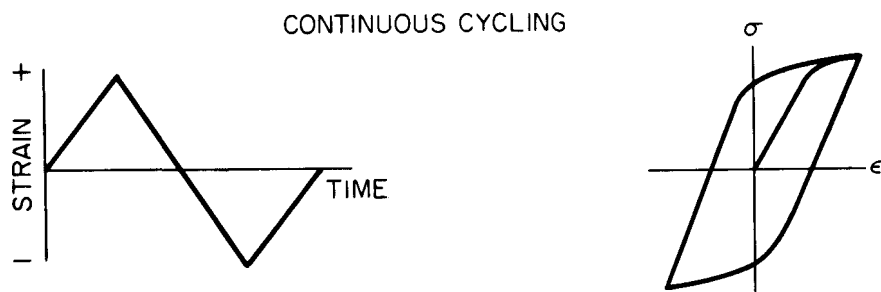


Fig. 3. Fully Reversed Strain-Controlled Continuous Cycling Fatigue Waveform.

The fatigue specimens were induction heated in air to either 427 or 538°C. Temperature was monitored and controlled from thermocouples spot-welded to the specimens at the locations shown in Fig. 1. Temperatures at the thermocouple locations were about 20°C lower than either test temperature at the minimum diameter of the hourglass specimens and about 80°C lower than at the 6.35-mm-diam gage section of the uniform-gage specimens. Control temperatures and consequently test temperatures were controlled to within $\pm 0.5^\circ\text{C}$. Temperature over the uniform gage section of the specimen shown in Fig. 1(b) was uniform within 5°C. Generally, the constant-amplitude, continuous cycling fatigue tests were performed in accordance with ASTM guidelines.¹ Additional details concerning experimental techniques can be found elsewhere.²

Subcritical crack growth tests were also performed on closed-loop electrohydraulic test machines. Tension-tension triangular waveform loading was used. The tests were conducted in air at 510°C in resistance furnaces. Thermocouples were attached to the specimens for continuous temperature monitoring throughout the test.

Crack length was measured visually with a measuring microscope on a micrometer slide. Recorded a vs N data (a = crack length; N = number of cycles) were computer-fitted with a second-degree polynomial equation. The rate of crack growth, da/dN , at a given N_i was obtained from the derivative of the parabolic equation. The value of ΔK (stress intensity factor range) associated with the da/dN value was computed from the fitted crack length a_i corresponding to N_i . The stress intensity factor equation for the compact tension specimen was

$$\Delta K = \frac{\Delta P}{B\sqrt{W}} \left[29.6 \left(\frac{a_i}{W} \right)^{0.5} - 18.5 \left(\frac{a_i}{W} \right)^{1.5} + 655.7 \left(\frac{a_i}{W} \right)^{2.5} - 1017 \left(\frac{a_i}{W} \right)^{3.5} + 638.9 \left(\frac{a_i}{W} \right)^{4.5} \right], \quad (1)$$

where

ΔP = cyclic load range (i.e. maximum-minimum load),

a_i = fitted crack length,

B = specimen thickness, and

W = specimen width.

For valid results the specimen had to be predominantly elastic for all values of applied load. By use of empirical relationships³ the uncracked alignment ($W - \alpha$) had to meet the following criterion:

$$(W - \alpha) = (4/\pi)(K_{max}/\sigma_{ys})^2 , \quad (2)$$

where

K_{max} = maximum stress intensity factor corresponding to the maximum load, and

σ_{ys} = 0.2% offset yield strength of the material at the test temperature.

Generally, subcritical crack growth tests were conducted according to ASTM-recommended practices.^{3,4} Additional experimental details have been reported previously.²

RESULTS AND DISCUSSION

Strain-Controlled Continuous Cycling Fatigue

Fully reversed strain-controlled continuous cycling fatigue tests were conducted on air-melt, VAR, and ESR heats (3P5601, 56447, and 91775, respectively) of 2 1/4 Cr-1 Mo steel, which had been given a simulated PWHT following an initial anneal or isothermal anneal treatment. Results of tests conducted to date at 427 and 538°C on each heat are given in Tables 4, 5, and 6. Generally, the tests were conducted at a constant strain rate of $4 \times 10^{-3}/s$, except in the high-cycle life range, where behavior is essentially elastic and permits load-controlled testing at frequencies of about 10 Hz. Tabulated values of total strain range, $\Delta\varepsilon_t$, were partitioned into elastic and plastic strain range components; that is $\Delta\varepsilon_t = \Delta\varepsilon_e + \Delta\varepsilon_p$. Elastic strain ranges were computed by dividing the stress range by the elastic modulus at the test temperature: $\Delta\varepsilon_e = \Delta\sigma/E$. The plastic strain range, $\Delta\varepsilon_p$, was then obtained by $\Delta\varepsilon_p = \Delta\varepsilon_t - \Delta\varepsilon_e$. Plastic strain ranges so calculated agreed well with measured widths of hysteresis loops of stress versus axial strain recorded during each test.

Table 4. Strain-Controlled Fatigue Data for 2 1/4 Cr-1 Mo Steel,^a Air-Melt Heat 3P5601

Specimen ^c	Total strain range, ^d $\Delta\epsilon_t$ (%)	Stress amplitude, ^b MPa		Stress range, $\Delta\sigma$ (MPa)	Strain range, ^b %		Cycles to failure, N_f	Time to failure, t_f (min)
		Tensile, σ_t	Compressive, σ_c		Plastic, $\Delta\epsilon_p$	Elastic, ^e $\Delta\epsilon_e$		
<u>Tests Conducted at 427°C</u>								
AP14	2.00	315	322	637	1.64	0.36	874	147
AP13	1.00	265	271	536	0.70	0.30	3,112	276
AP08	0.52	222	228	450	0.27	0.25	22,700	1,002
AP10	0.40	213	214	427	0.16	0.24	112,028	3,984
AP01	0.30	194	196	390	0.08	0.22	1,858,212	49,038
AP02U	0.25	171	178	349	0.06	0.19	1,339,362	27,816
<u>Tests Conducted at 538°C</u>								
AP03	2.00	254	259	513	1.67	0.33	754	126
AP07	1.00	219	224	443	0.71	0.29	2,495	220
AP12	0.50	184	186	371	0.26	0.24	19,809	876
AP16	0.42	179	179	359	0.19	0.23	41,500	1,476
AP01T	0.40	174	178	352	0.17	0.23	76,263	2,706
AP11	0.32	162	164	326	0.11	0.21	272,490	7,314
AP04U	0.25	172	186	358	0.13	0.12	1,771,665	8,802

^aMaterial was annealed and postweld heat-treated.

^bValues at $N_f/2$.

^cU implies uniform-gage specimen (6.35 mm in diameter with a gage length of 19.0 mm). All others were hourglass specimens (6.35 mm minimum in diameter with a radius-to-diam ratio of 6).

^dTests were conducted at a constant strain rate of $4 \times 10^{-3}/s$. Tests with $\Delta\epsilon_t < 0.3\%$ were switched from strain to load control when the cyclic stress reached a stabilized value, and the test frequency was increased to about 10 Hz.

^eModulus of Elasticity, $E = 179$ GPa at 427°C; $E = 155$ GPa at 538°C.

∞

Table 5. Strain-Controlled Fatigue Data for 2 1/4 Cr-1 Mo Steel,^a VAR-Melt Heat 56447

Specimen ^c	Total strain range, ^d $\Delta\epsilon_t$ (%)	Stress amplitude, ^b MPa		Stress range, $\Delta\sigma$ (MPa)	Strain range, ^b %		Cycles to failure, N_f	Time to failure, t_f (min)
		Tensile, σ_t	Compressive, σ_c		Plastic, $\Delta\epsilon_p$	Elastic, ^e $\Delta\epsilon_e$		
<u>Tests Conducted at 427°C</u>								
VPH09	2.00	317	317	634	1.65	0.35	899	150
VPH06	1.00	269	272	541	0.70	0.30	3,193	266
VPH01	0.50	228	231	459	0.27	0.26	23,230	968
VPH08	0.40	214	221	435	0.16	0.24	77,590	2,586
VPH04	0.30	183	193	376	0.09	0.21	2,437,505	39,174
VPU12	0.25	190	186	376	0.04	0.21	811,045	16,842
<u>Tests Conducted at 538°C</u>								
VPH13	2.00	250	260	519	1.67	0.33	688	115
VPH14	1.00	224	228	452	0.71	0.29	2,160	192
VPH12	0.53	179	183	362	0.30	0.23	11,464	507
VPH15	0.40	165	169	334	0.18	0.22	71,417	2,628
VPH16	0.30	159	170	329	0.09	0.21	585,419	14,636
VPU07	0.25	147	144	291	0.06	0.19	501,075	10,439
VPU08	0.25	172	200	372	0.01	0.24	587,096	3,480
VPU10	0.20	145	141	286	0.02	0.18	26,076,400 ^f	

^aMaterial was annealed and postweld heat-treated.

^bValues at $N_f/2$.

^cH implies hourglass specimen (6.35 mm minimum in diameter with a radius-to-diam ratio of 6); U implies uniform gage specimen (6.35 mm in diameter with a gage length of 19.0 mm).

^dTests conducted at a constant strain rate of 4×10^{-3} /s. Tests with $\Delta\epsilon_t < 0.3\%$ were switched from strain to load control and test frequency was increased to about 10 Hz.

^eDynamic Modulus of Elasticity, $E = 179$ GPa at 427°C; $E = 155$ GPa at 538°C.

^fTest discontinued.

Table 6. Strain-Controlled Fatigue Data for 2 1/4 Cr-1 Mo Steel,^a ESR-Melt Heat 91775

Specimen	Total strain range, ^c $\Delta\epsilon_t$ (%)	Stress amplitude, ^b MPa		Stress range (MPa)	Strain range, ^b %		Cycles to failure, N_f	Time to failure, t_f (min)
		Tensile, σ_t	Compressive, σ_c		Plastic, $\Delta\epsilon_p$	Elastic, $\Delta\epsilon_e$		
<u>Tests Conducted at 427°C</u>								
EH5	3.15	331	352	683	2.77	0.38	340	57.0
EH8	1.53	260	273	533	1.24	0.29	1,097	96.0
EH1	0.78	236	246	482	0.51	0.27	5,518	246.0
EH9	0.77	250	253	503	0.49	0.28	5,000	222.0
EH2	0.47	198	208	406	0.24	0.23	74,219	1,956.0
EH4	0.31	180	192	372	0.10	0.21	949,260	16,875.0
<u>Tests Conducted at 538°C</u>								
EH10	3.24	284	309	593	2.86	0.38	328	54.0
EH11	1.47	207	220	427	1.19	0.28	839	72.0
EH12	0.78	172	210	382	0.53	0.25	3,062	135.0
EH6	0.46	160	166	326	0.25	0.21	18,403	486.0
EH3	0.46	160	153	313	0.26	0.20	20,075	528.0
EH7	0.31	146	163	309	0.11	0.20	74,118	1,380.0

^aMaterial was isothermally annealed and postweld heat-treated.

^bValues at $N_f/2$.

^cTests conducted at a constant strain rate of about 6×10^{-3} /s on hourglass specimens (6.35 mm in diameter with radius-to-diam ratio of 6).

^dDynamic modulus of elasticity, $E = 179$ GPa at 427°C; $E = 155$ GPa at 538°C.

Elastic, plastic, and total strain ranges are plotted against cycles to failure in Figs. 4 and 5 for 427 and 538°C respectively. The fatigue behavior apparently does not differ for the heats of material obtained by the three different melting practices (i.e. air-melt, VAR, and ESR).

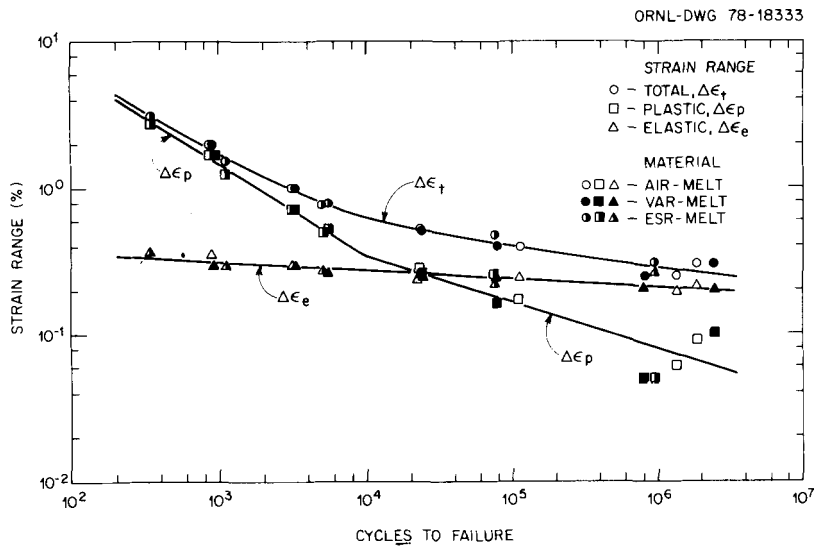


Fig. 4. Total, Elastic, and Plastic Strain Ranges vs Cycles to Failure for Postweld Heat-Treated 2 1/4 Cr-1 Mo Steel at 427°C.

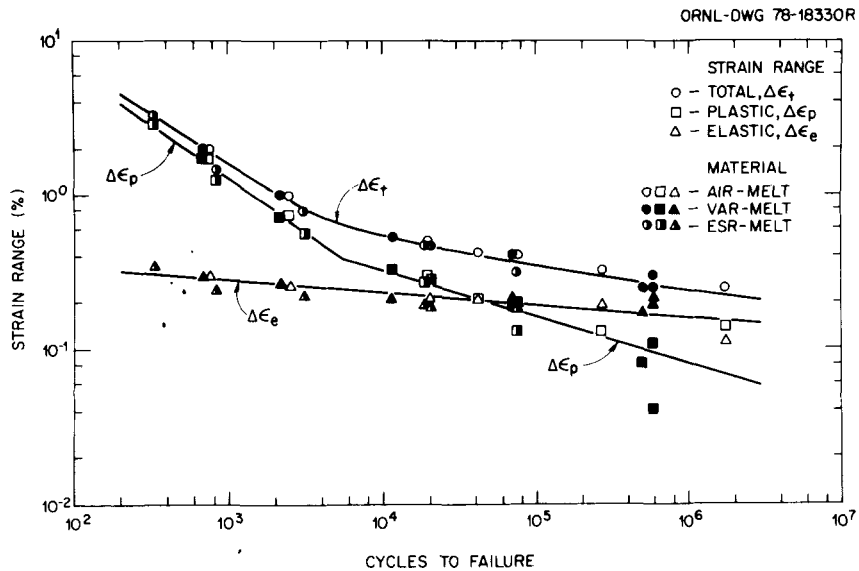


Fig. 5. Total, Elastic, and Plastic Strain Ranges vs Cycles to Failure for Postweld Heat-Treated 2 1/4 Cr-1 Mo Steel at 538°C.

One of the most common methods⁵ of fitting fatigue data uses power-law relationships between cycles to failure and the elastic and plastic strain range component. Thus,

$$\Delta\epsilon_e = AN_f^{-\alpha}, \quad (3)$$

$$\Delta\epsilon_p = BN_f^{-\beta}, \quad (4)$$

so that

$$\Delta\epsilon_t = AN_f^{-\alpha} + BN_f^{-\beta}. \quad (5)$$

In general, data for annealed and isothermally annealed 2 1/4 Cr-1 Mo steel² show that B and β have one set of values in the low-cycle region and another in the high-cycle region, so a log-log plot of $\Delta\epsilon_p$ vs N_f is bilinear rather than linear. Table 7 summarizes the results of fitting these relationships to the interim data for the postweld heat-treated 2 1/4 Cr-1 Mo steel.

Table 7. Coefficients and Exponents of Power-Law Fits for Postweld Heat-Treated 2 1/4 Cr-1 Mo Steel

Temperature (°C)	N_f range ^a (cycles)	Values of constants in $\Delta\epsilon_t = AN_f^{-\alpha} + BN_f^{-\beta}$			
		A	α	B	b
427	<10,000	0.474	0.060	108.78	0.625
427	>10,000	0.474	0.060	6.60	0.321
538	<5,000	0.484	0.80	166.34	0.704
538	>5,000	0.484	0.80	4.72	0.293

^aNear the switchover use the equation which yields the higher $\Delta\epsilon_p$ at a given N_f . Switchover occurs at about $\Delta\epsilon_p = 0.35\%$ for both temperatures.

Fully reversed strain-controlled continuous cycling fatigue properties of annealed and isothermally annealed 2 1/4 Cr-1 Mo steel have been reported in some detail.^{2,6-8} Power-law fits⁹ of data that encompass

several air-melt heats of material are listed in Table 8. The effects of specimen geometry on fatigue life are discussed in the Appendix. The interim data on postweld heat-treated air-melt, VAR, and ESR material

Table 8. Coefficients and Exponents of Power-Law Fits for Annealed and Isothermally Annealed 2 1/4 Cr-1 Mo Steel

Maximum Temperature (°C)	N_f range ^a	Values of constants in $\Delta\epsilon_t = AN_f^{-\alpha} + BN_f^{-\beta}$			
		A	α	B	β
427	<10,000	0.594	0.067	156.50	0.658
	>10,000	0.594	0.067	187.59	0.732
593	<5,000	0.484	0.065	19.37	0.418
	>5,000	0.484	0.065	12.12	0.398

from Tables 4, 5, and 6 are compared with the fatigue behavior of annealed and isothermally annealed air-melt 2 1/4 Cr-1 Mo at 427 and 538°C in Figs. 6 and 7. Apparently neither heat-to-heat variations, melting practice, or heat treatment affect cyclic life at either temperature. High-cycle tests on the postweld heat-treated material are continuing to obtain data to about 10^8 cycles to failure.

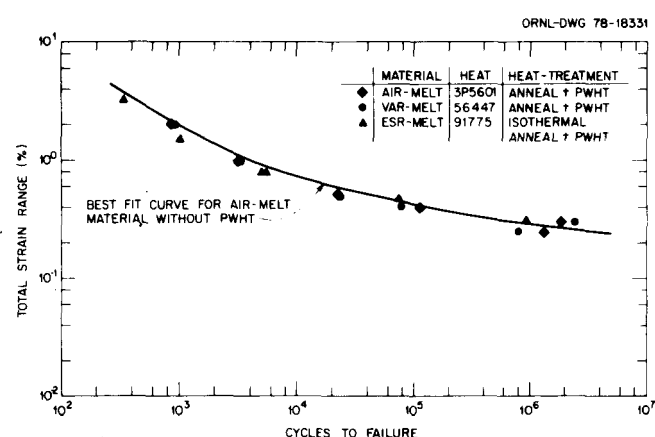


Fig. 6. Comparison of Data at 427°C on Postweld Heat-Treated Air-Melted, Vacuum-Remelt, and Electroslag Remelt Material with the Best Fit Curve for Annealed and Isothermally Annealed 2 1/4 Cr-1 Mo Steel.

ORNL-DWG 78-18332

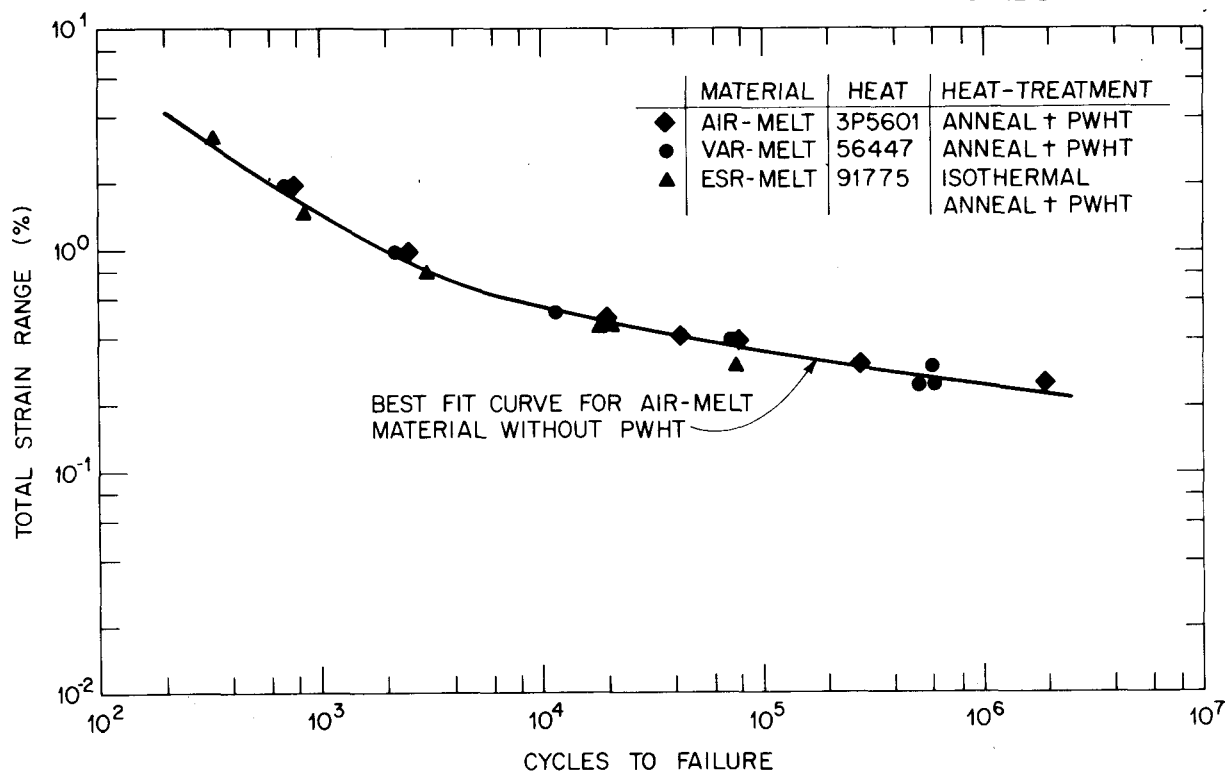


Fig. 7. Comparison of Data at 538°C on Postweld Heat-Treated Air-Melt, Vacuum-Remelt, and Electroslag Remelt Material with the Best Fit Curve for Annealed and Isothermally Annealed 2 1/4 Cr-1 Mo Steel.

Fatigue Crack Growth Rate

Fatigue crack growth in isothermally annealed air-melted 2 1/4 Cr-1 Mo steel has been reported in some detail.^{2,8,10} We examined fatigue crack growth rate (FCGR) as a function of stress intensity, temperature (-101 to 593°C), frequency, mean stress, heat-to-heat variations, and environment. Most of these data were obtained at 510°C. Additional tests are being conducted at 510°C to provide data at higher stress intensity levels and to investigate the frequency dependence of mean stress effects on crack growth rates. Also, FCGR of postweld heat-treated VAR material will be compared to crack growth behavior of air-melted 2 1/4 Cr-1 Mo steel. These tests are described in Table 9.

Table 9. Test Matrix for Fatigue Crack Growth Rate Tests of 2 1/4 Cr-1 Mo Steel at 510°C

Material	Heat treatment ^a	Frequency (Hz)	Hold time (min)	R	ΔK Range MPa \sqrt{m}	Environment	Status ^b
Air-melt (C-6534-10H)	Isothermal anneal	0.0067	0	0.05	15-55	Air	
		0.0067	0	0.5	10-28		P
		0.067	0	0.05	30-55		C
		0.67	0	0.05	30-55		C
		0.67	0	0.5	18-28		C
		0.0067	1	0.05	15-30		
VAR (56447)	Anneal + PWHT	0.0067	0	0.05	15-55	Air	
		0.067	0	0.05	15-55		
Air-melt (C-6534-10H)	Isothermal anneal	0.067	0	0.05	15-55	Steam	
		0.067	0	0.5	10-28		

^aSee Table 3 for description of heat treatment.^bC - complete; P - in progress. Status as of November 1, 1978.

Previously reported results in Fig. 8 show that crack growth rate increased monotonically with each decrease in frequency at 510°C. Results of additional tests at frequencies of 0.067 and 0.67 Hz have extended data to stress levels of about 57 MPa \sqrt{m} and agree well with previous results.

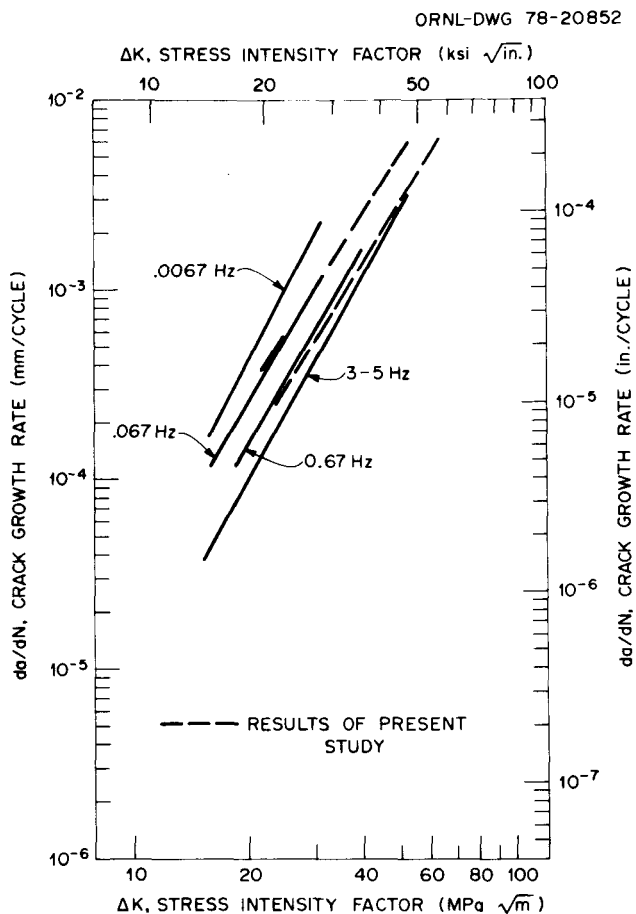


Fig. 8. Effect of Frequency on the Fatigue Crack Growth Rate of Isothermally Annealed 2 1/4 Cr-1 Mo Steel Tested at 510°C in Air with $R = 0.05$. Results of recent tests at high ΔK are included.

The effect of mean stress on FCGR is shown in Fig. 9(a). Under all conditions examined an increase in the level of mean stress as measured by $R = K_{min}/K_{max}$ increased the growth rate at a given level of stress intensity range, ΔK .

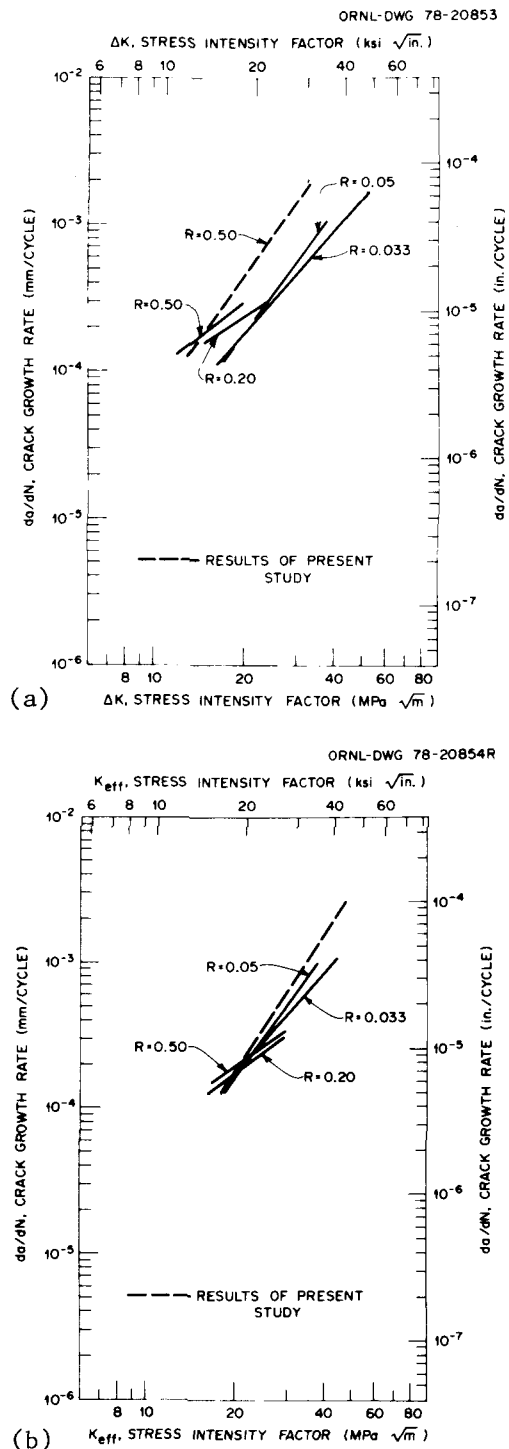


Fig. 9. Effect of Mean Stress on the Fatigue Crack Growth Rate of Isothermally Annealed 2 1/4 Cr-1 Mo Steel in Air at 510°C. (a) Crack growth rate plotted as a function of ΔK . (b) Growth rate plotted as a function of $K_{eff} = K_{max} (1 - R)^{0.5}$.

Mean stress effects on crack growth are frequently correlated by use of an effective stress intensity factor, K_{eff} .¹¹ By use of crack closure argument, K_{eff} is :

$$K_{eff} = K_{max} (1 - R)^{0.5} . \quad (6)$$

The data in Fig. 9(a) have been replotted in terms of K_{eff} in Fig. 9(b). Comparing (Figs. 9(a) and (b)), apparently the data consolidate somewhat. However, indications of slope divergence at the various R levels remain, particularly if we attempt extrapolation. We need additional data to further confirm the use of this approach for mean stress effects on this material.

CONCLUSIONS

Results of fully reversed continuous cycling strain-controlled fatigue and fatigue crack growth tests of 2 1/4 Cr-1 Mo steel were reported. Air-melt, VAR, and ESR heats, annealed or isothermally annealed with a final PWHT, showed no apparent difference in strain range vs cycles to failure at either 427°C or 538°C. Fatigue resistance of the PWHT material is similar to that of annealed and isothermally annealed material.

Interim results of fatigue crack growth rate (FCGR) tests at 510°C extended previous data to higher stress intensity levels. Data on FCGR at frequencies of 0.067 and 0.67 Hz obtained over a stress intensity range of 30 to 60 MPa \sqrt{m} agreed well with previous results at 20 to 40 MPa \sqrt{m} . A test conducted for a mean stress level of $R = 0.5$ ($R =$ minimum load/maximum load) has extended previous data from 15 to 20 MPa \sqrt{m} to 60 MPa \sqrt{m} giving results comparable with available results for mean stress levels of $R = 0.033-0.05$.

ACKNOWLEDGMENTS

The authors gratefully acknowledge the assistance of L. K. Egner and E. Bolling in conducting the experimental tests, K. C. Liu and W. J. Stelzman for reviewing the paper, B. Ashdown for editing the paper, and K. A. Witherspoon for typing the manuscript.

REFERENCES

1. ASTM Standard E 606-77T, "Practice for Constant-Amplitude Low-Cycle Fatigue Testing."
2. C. R. Brinkman, M. K. Booker, J. P. Strizak, W. R. Corwin, J. L. Frazier, and J. M. Leitnaker, *Interim Report on the Continuous Cycling Elevated Temperature Fatigue and Subcritical Crack Growth Behavior of 2 1/4 Cr-1 Mo Steel*, ORNL-TM-4993 (December 1975).
3. S. J. Hodak, Jr., and A. Saxena, *Development of Standard Methods of Testing and Analyzing Fatigue Crack Growth Rate Data--Third Semi-Annual Report*, Research Report 77-9E7-AFCGR-R1, Westinghouse Research Laboratories, Pittsburgh (March 1977).
4. ASTM Standard E 399-74, "Standard Test Method for Plane-Strain Fracture Toughness of Metallic Materials."
5. S. S. Manson, "Fatigue: A Complex Subject — Some Simple Approximations," *Exp. Mech.* 5(7): 193-226 (July 1965).
6. C. R. Brinkman, M. K. Booker, J. P. Strizak, and W. R. Corwin, "Elevated Temperature Fatigue Behavior of 2 1/4 Cr-1 Mo Steel," *Trans. ASME* 97(4): 252-57 (1975).
7. M. K. Booker, T. L. Hebble, D. O. Hobson, and C. R. Brinkman, "Mechanical Property Correlation for 2 1/4 Cr-1 Mo Steel in Support of Nuclear Reactor Systems Design," *Inst. J. Pres. Ves. and Piping* 5(3): 181-205 (1977).
8. C. R. Brinkman, W. R. Corwin, M. K. Booker, T. L. Hebble, and R. L. Klueh, *Time-Dependent Mechanical Properties of 2 1/4 Cr-1 Mo Steel for Use in Steam Generator Design*, ORNL-5125 (March 1976).

9. M. K. Booker, "Strain-Controlled Fatigue of 2 1/4 Cr-1 Mo Steel," *Mechanical Properties Test Data for Structural Materials Quart. Prog. Rep. April 30, 1978*, ORNL-5416 (June 1978), pp. 145-61.
10. W. R. Corwin, M. K. Booker, B.L.P. Booker, and C. R. Brinkman, *Fatigue Crack Propagation in 2 1/4 Cr-1 Mo Steel*, ORNL-5355 (February 1978).
11. E. K. Walker, "An Effective Strain Concept for Crack Propagation and Fatigue Life with Specific Applications to Biaxial Stress Fatigue," p. 225 in *Proc. Air Force Conf. Fatigue and Fracture of Aircraft Structures and Materials*, ed. by H. A. Wood et al., AFFDL-TR-70-144, 1970.

APPENDIX

Blank Page

THE EFFECT OF SPECIMEN GEOMETRY ON FATIGUE LIFE

INTRODUCTION

A recent American Society for Testing and Materials (ASTM) tentative recommended¹ that low-cycle fatigue tests use hourglass and uniform-gage test specimens with solid circular crosssections and minimum diameters of 6.35 mm in the test section. These specimens were selected because of their predominance in the published low-cycle fatigue data. Specimens of other diameters or configurations can be successfully tested under the ASTM guidelines; however, the experimentalist is cautioned that crack growth rate, test-material grain size, and other considerations might preclude direct comparisons with the results for the recommended specimens. The ASTM-recommended hourglass and uniform-gage specimens as well as a second hourglass specimen scaled down from the ASTM specimen with a 5.08-mm-diam in the test section have been commonly used at ORNL. The smaller specimen has been particularly useful when product form has been a limitation. Recent reports^{2,3} indicate that specimen geometry significantly influences results of fatigue tests. Observations concerning the effect of specimen geometry on fatigue life are presented in this appendix.

RESULTS AND DISCUSSION

We directly compared the results from the 6.35-mm-diam ASTM-recommended hourglass and uniform-gage specimens and the smaller 5.05-mm-diam hourglass specimen for a single heat (3P5601) of isothermally annealed 2 1/4 Cr-1 Mo steel plate. Chemical composition and heat treatment of the material and experimental procedures were discussed earlier in the report. Results of fully reversed continuous cycle strain-controlled push-pull fatigue tests are given in Table A1, while fatigue life at 538°C is plotted as a function of both strain range and specimen geometry in Fig. A1.

Table Al. Continuous Cycling Fatigue Data for Isothermally Annealed 2 1/4 Cr-1 Mo Steel, Heat 3P5601, Tested at 538°C, Employing Several Specimen Geometries

Specimen geometry ^b	Specimen number	Total strain range, $\Delta\epsilon_t$	Values at $N_f/2$					Cycles to failure, N_f	Time to failure, t_F (h)
			Stress range $\Delta\sigma$ (MPa)	Tensile stress amplitude σ_t (MPa)	Compressive stress amplitude σ_c (MPa)	Strain range, %	Elastic $\Delta\epsilon_e$ (%)		
6H	MIL-21	2.00	563	257	306	0.30	1.70	881	2.4
6H	BIL-16	2.09	549			0.36	1.73	846	2.4
6H	BIL-15	1.03	467			0.30	0.73	2,477	3.5
6H	MIL-10	0.50	391	192	199	0.22	0.28	16,036	11.1
6H	BIL-11	0.50	427			0.23	0.27	16,185	11.2
5H	ITL-135	2.00	607	293	314	0.36	1.64	692	1.9
5H	ITL-134	1.00	511	259	252	0.33	0.67	2,377	3.5
5H	ITL-133	0.50	440	221	219	0.22	0.28	26,611	19.6
5H	ITL-17	0.50	386	189	197	0.22	0.28	15,164	10.5
5H	ITT-7	0.38	414	209	206	0.24	0.14	63,906	33.7
U	IUL-10	1.99	558	274	284	0.32	1.67	679	1.9
U	IUL-8	0.97	477	238	239	0.27	0.70	2,000	2.8
U	MIL-31U	0.50	393	198	195	0.22	0.28	9,353	6.5
U	IUL-6	0.50	412	204	208	0.24	0.26	10.764	7.5
U	IUL-7	0.35	393	197	196	0.22	0.13	73,256	35.6

^aFully reversed strain-controlled tests conducted at a constant strain rate of $4 \times 10^{-3} \text{ s}^{-1}$.

^b6H, hourglass specimen with a minimum diam = 6.45 mm and $R/D = 6$; 5H, hourglass specimen with a minimum diam = 5.08 mm and $R/D = 6$; and U, 6.35-mm-diam uniform-gage specimen.

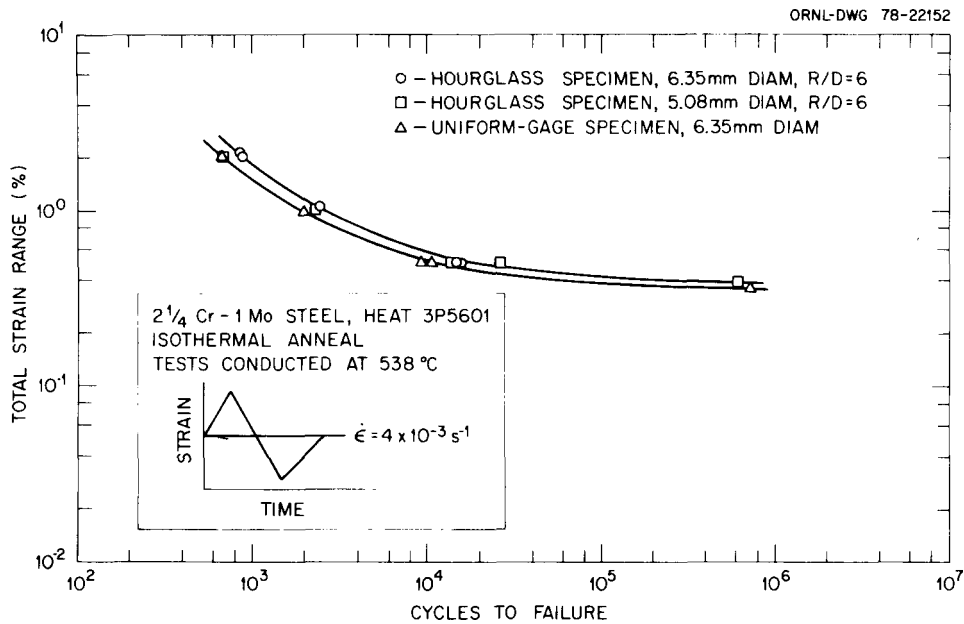


Fig. A1. Fatigue Life of 2 1/4 Cr-1 Mo Steel as a Function of Both Strain Range and Test Specimen Geometry.

Several discrepancies are apparent in the results from the various specimen geometries.

Comparison of 6.35-mm-Diam Hourglass-Shaped and Uniform-Gage Specimens

Figure A1 shows that for a given strain range uniform-gage specimens generally have a lower fatigue life than hourglass specimens of the same diameter. The discrepancy in the results from these specimens does not appear to be due to modes of strain measurement. Axial strain in the test section of the uniform-gage specimen is commonly measured directly with an axial extensometer; for hourglass specimens diametral strain measurement is used to compute axial strain (ϵ_a) according to the following equation:

$$\epsilon_a = \frac{\Delta\sigma}{E} \left(1 - \frac{v_e}{v_p}\right) + \frac{\Delta\varepsilon_d}{v_p} , \quad (A1)$$

where

v_e = Poisson's ratio for elastic strain,

v_p = Poisson's ratio for plastic strain,

E = modulus of elasticity,

$\Delta\sigma$ = nominal stress range, and

$\Delta\varepsilon_d$ = diametral strain obtained from the diametral extensometer.

Dewey² has shown by finite element analysis that errors in axial and diametral extensometry for the specimens are less than 2 to 3% and tend to decrease as strain increases. Further, Bui-Quoc and Biron³ have observed that at a given strain range the number of cycles to failure for continuous cycle fatigue tests of 304 stainless steel using uniform-gage specimens was practically the same under axial and diametral modes of strain measurement.

The accuracy of axial strain computed from Eq. (A1) depends on using the correct values of ν_p and the elastic material constants E and ν_e . Values of E and ν_e are generally obtained from tensile test results, while ν_p is equal to 0.5, assuming that the volume of a metal under large plastic deformation in a tension test remains constant. All three material properties presumably remain constant during a fatigue test.

However, Bui-Quoc and Biron³ have shown that ν_p decreases slightly during cyclic loading and suggest that a value of 0.48 might be more appropriate than the assumed 0.50. Extensometry error and optimization of ν_p account for less than a 5% overestimate of computed axial strain for hourglass specimens in the low-cycle fatigue region. Even if this correction factor was applied to the results shown in Fig. A1, the fatigue life of hourglass specimens would still be consistently higher than that of uniform-gage specimens of the same diameter. These results suggest that specimen geometry (i.e., hourglass versus uniform gage of the same diameter) significantly influences fatigue life.

The discrepancy in the results for the two types of specimens may have several causes. The hourglass and uniform-gage specimen geometries have been critically examined by both Dewey² and Schultz⁴ by means of inelastic finite element techniques. Stress and strain distributions over the cross section of the uniform-gage specimen are essentially uniform within the ASTM-recommended extensometer length. On the other hand, triaxial stress and nonuniformity of diametral strain exist in the test section of the hourglass specimen. However, the multiaxiality of stress is low and will probably not greatly affect

fatigue life. Since the uniform-gage specimen has a larger volume exposed to maximum strain than the hourglass specimen, surface flaws, particularly at low-strain ranges, probably influence fatigue more in the uniform-gage specimen. Schultz further determined that the hourglass specimen does not adequately obtain cyclic stress-strain data since it underestimates the strain for a given stress; whereas results from the uniform-gage specimen agreed excellently with the stress-strain curve predicted according to constitutive theory.

Indeed, the response of the two specimens differs. As shown in Fig. A2 cycling specimens in strain control generally resulted in initial cyclic hardening followed by gradual hardening, softening, or near

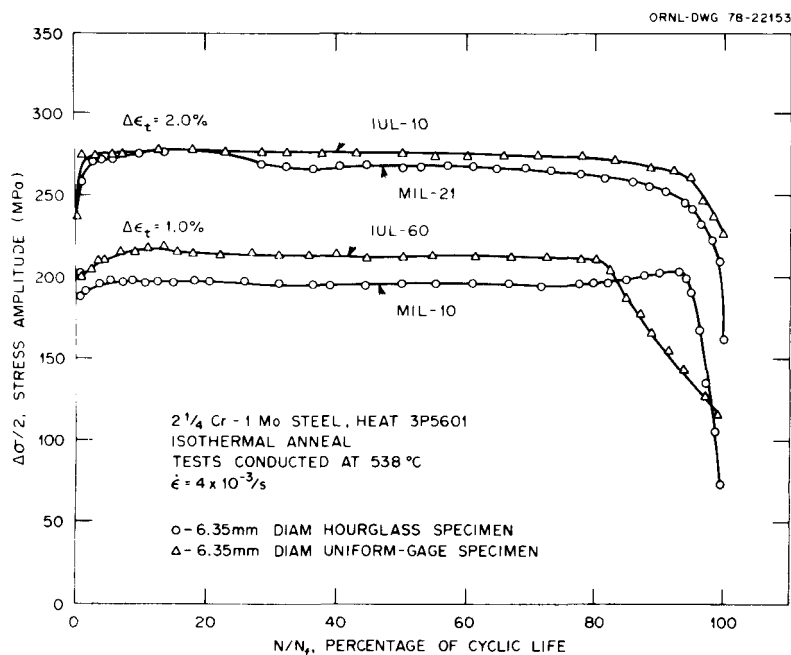


Fig. A2. Stress Amplitude vs Fraction of Cyclic Life for Continuous Cycling Fatigue Tests Using Uniform-Gage and Hourglass Test Specimens.

stability as cycling continued, as evidenced by changes in load required to maintain the prescribed total axial strain range constant. However, the uniform-gage specimen reached a higher half-life stress value than hourglass specimens of the same diameter. Since the number of cycles to failure is closely related to the applied cyclic stress, we expect that the uniform-gage specimens would have correspondingly lower

lives. Bui-Quoc and Biron³ made the same observation from low-cycle fatigue results for type 304 stainless steel using 12.70-mm-diam uniform-gage and hourglass specimens.

Comparison of 5.08-mm and 6.35-mm-Diam Hourglass Specimens

Limited comparisons between fatigue results obtained from both 5.08-mm and 6.35-mm-diam hourglass specimens indicate that specimen size (diameter) affects fatigue life. As shown in Table A1 and Fig. A1, the 5.08-mm-diam specimens tend to develop a higher half-life ($N_f/2$) stress range for a given total axial strain range and consequent lower fatigue life than the 6.35-mm-diam specimen. However, the difference in the response of the two specimens tends to decrease with decreasing total axial strain range. According to Dewey,² finite element analysis would not predict this discrepancy for two proportionately sized specimens.

CONCLUSIONS

Limited comparisons of low-cycle fatigue results obtained from commonly used specimens indicate that specimen geometry (hourglass and uniform-gage types) and specimen size (diameter) significantly influence fatigue life.

1. Results of continuous cycle fatigue tests for 2 1/4 Cr-1 Mo steel at 538°C using ASTM-recommended 6.35-mm-diam hourglass-shaped and uniform-gage specimens showed that uniform-gage specimens develop a higher stress range for a given total axial strain range and consequently have a lower fatigue life than hourglass-shaped specimens.

2. Results from proportionately sized 5.08-mm and 6.35-mm-diam hourglass specimens showed that the smaller specimen develops a higher stress range and consequently has a lower fatigue life than the larger specimen. The discrepancy in the results for the two specimens tends to decrease with decreasing total axial strain range.

REFERENCES

1. ASTM E 606-77T, "Practice for Constant Amplitude Low-Cycle Fatigue Testing."
2. B. R. Dewey, "Finite-Element Analysis of Creep and Plasticity Tensile-Test Specimens," *Exp. Mech.* 16(1): 16-20 (1976).
3. T. Bui-Quoc and A. Biron, "Comparison of Low-Cycle Fatigue Results with Axial and Diametral Extensometers," *Exp. Mech.* 18(4): 127-33 (1978).
4. C. C. Schultz and H. M. Zien, "Verification of Specimens for Low Cycle Fatigue and Cyclic Plasticity Testing," paper presented at the Energy Technology Conference and Exhibit, ASME 77-PVP-35, Houston, Texas, September 18-22, 1977.

Blank Page

ORNL/TM-6782
Distribution
Category UC-79b, -h, -k

INTERNAL DISTRIBUTION

1-2. Central Research Library	23. R. L. Klueh
3. Document Reference Section	24. K. C. Liu
4-5. Laboratory Records Department	25. C. E. Pugh
6. Laboratory Records Department, RC	26. G. M. Slaughter
7. ORNL Patent Section	27. J. H. Smith
8. J. J. Blass	28-32. J. P. Strizak
9. M. K. Booker	33. R. W. Swindeman
10-14. C. R. Brinkman	34. T. Weerasooriya
15. J. M. Corum	35. R. W. Balluffi (Consultant)
16. J. R. DiStefano	36. A. L. Bement, Jr. (Consultant)
17. J. R. Ellis	37. W. R. Hibbard, Jr. (Consultant)
18. R. J. Gray	38. E. H. Kottcamp, Jr. (Consultant)
19-21. M. R. Hill	39. M. J. Mayfield (Consultant)
22. J. F. King	40. J. T. Stringer (Consultant)

EXTERNAL DISTRIBUTION

41-42. DOE DIVISION OF REACTOR RESEARCH AND TECHNOLOGY, Washington, DC 20545
Director

43. DOE OAK RIDGE OPERATIONS OFFICE, P.O. Box E, Oak Ridge, TN 37830
Assistant Manager, Energy Research and Development

44-304. DOE TECHNICAL INFORMATION CENTER, Office of Information Services,
P.O. Box 62, Oak Ridge, TN 37830
For distribution as shown in TID-4500 Distribution Category,
UC-79b (Fuels and Materials Engineering Development);
UC-79h (Structural Materials Design Engineering);
UC-79k (Components)